**Proceedings of the ASME 2018 Pressure Vessels and Piping Conference**
**PVP2018**
**July 15-20, 2018, Prague, Czech Republic**

# PVP2018-84979

# ISSUES WITH MULTIAXIAL FATIGUE ASSESSMENT IN THE ASME BOILER AND PRESSURE VESSEL CODE

**Marco Antonio Meggiolaro**
**Jaime Tupiassú Pinho de Castro**
Pontifical Catholic University of Rio de Janeiro
Rio de Janeiro, RJ, Brazil

**Hao Wu**
School of Aerospace Engineering and Applied Mechanics, Tongji University
Shanghai, P.R. China

## ABSTRACT

This work analyzes the applicability of the ASME Boiler and Pressure Vessel Code procedures to calculate fatigue crack initiation under multiaxial stresses and/or strains, in particular when caused by non-proportional loads that lead the principal directions at the critical point to vary with time, e.g. due to out-of-phase bending and torsion loads induced by independent sources. Classic uniaxial fatigue damage models are usually inappropriate for analyzing multiaxial loads, since they can generate highly inaccurate predictions. Moreover, it is shown that the ASME procedures can lead to *non-conservative* results for non-proportional load histories.

## INTRODUCTION

Service loads can be applied on one or on several points of a structural component. They can be generated by only one or by multiple sources, coherent or not. In general, such loads cause bending, torsion, normal, and/or shear efforts which, when combined, can (and usually do) generate multiaxial strains and stresses at the critical point(s) of the component. Multiaxial fatigue deals with the initiation and/or the propagation of fatigue cracks under such general conditions.

Multiaxial fatigue load histories can be *proportional* or *non-proportional* (NP). They are proportional when the principal axes of the stresses and strains induced by them, and thus their maximum-shear planes, remain fixed during their entire duration. On the other hand, NP loads induce principal stress/strain directions that change in time (1).

Consider for instance a tension-torsion problem where a shaft is loaded by a normal stress $\sigma_x(t)$ in the **x** direction combined with a shear stress $\tau_{xy}(t)$, where **t** stands for time. In this case, the principal stresses $\sigma_1$ and $\sigma_2$ and the angle $\theta_1$ between $\sigma_1$ and the **x** axis are given by

$$\sigma_{1,2} = \frac{\sigma_x}{2} \pm \sqrt{\left(\frac{\sigma_x}{2}\right)^2 + \tau_{xy}^2} \quad \text{and}$$
$$\theta_1(t) = \frac{1}{2}\tan^{-1}\left[\frac{2\tau_{xy}(t)}{\sigma_x(t)}\right] \qquad (1)$$

When the shear and normal stresses are proportional, the ratio $\tau_{xy}(t)/\sigma_x(t)$ and the angle $\theta_1(t)$ remain fixed for all time **t**, thus this simple multiaxial loading history is proportional. If $\tau_{xy}(t)/\sigma_x(t)$ and hence $\theta_1(t)$ vary with time, then the loading is non-proportional. The relative degree of non-proportionality of any multiaxial load history is quantified by its so-called non-proportionality factor $0 \le F_{NP} \le 1$, with $F_{NP} = 0$ standing for a proportional load history and $F_{NP} = 1$ for a fully NP history.

If all stress and strain components are periodic and have the same frequency, they can also be classified as *in-phase* or *out-of-phase*. Figure 1 shows in-phase as well as $90^o$ and $180^o$ out-of-phase tension-torsion load histories. Both the in-phase and the $180^o$ out-of-phase loadings have a constant $\tau_{xy}(t)/\sigma_x(t)$ ratio, so they are proportional histories with $F_{NP} = 0$. The $90^o$ out-of-phase tension-torsion loading, on the other hand, always results in a NP history, with the $F_{NP}$ value depending on the ratio between the shear and normal amplitudes. It is usually accepted (1) that, in tension-torsion histories, the maximum value $F_{NP} = 1$ is achieved for sinusoidal $90^o$ out-of-phase loadings with equal amplitudes for $\sigma_x$ and $\tau_{xy}\sqrt{3}$, when the von Mises stress $\sqrt{\sigma_x^2 + 3\tau_{xy}^2}$ remains constant along the load path.

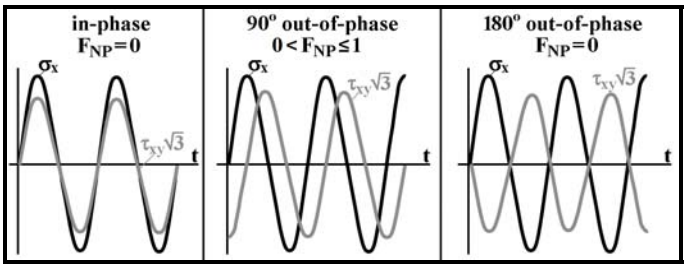


Fig. 1: In-phase, **90°** out-of-phase and **180°** out-of-phase tension-torsion histories.

The $\mathbf{F_{NP}}$ value of tension-torsion loads can also be obtained from the shape of their stress paths represented in the von Mises tension-torsion diagram $\sigma_x \times \tau_{xy}\sqrt{3}$, where the distance between any stress state and the diagram origin is equal to $\sigma_{Mises} = \sqrt{\sigma_x^2 + 3\tau_{xy}^2}$, see Fig. 2. For zero mean loads, $\mathbf{F_{NP}}$ is usually estimated from the aspect ratio **b/a** of an ellipse that encloses the stress path, where **a** and **b** ≤ **a** are the ellipse semi-axes. So, both in-phase and **180°** out-of-phase tension-torsion loadings, which always result in straight stress paths, are also always proportional and have $\mathbf{F_{NP} = 0}$ under zero mean loads, see Fig. 2(left). For sinusoidal **90°** out-of-phase loadings with equal amplitudes for $\sigma_x$ and $\tau_{xy}\sqrt{3}$, the resulting tension-torsion path describes a circle, hence it induces $\mathbf{F_{NP} = b/a = 1}$ as expected, see Fig. 2(middle). Figure 2(right) shows the enclosing ellipse of a general periodic history, associated with a NP factor such that $\mathbf{0 \leq F_{NP} \leq 1}$.

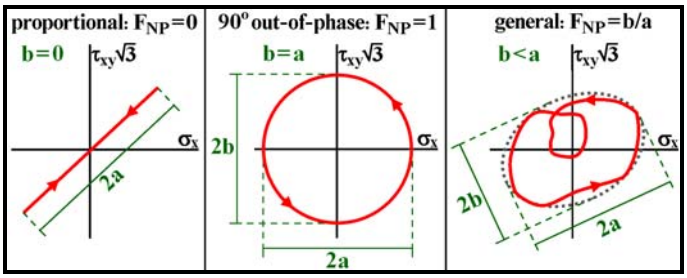


Fig. 2: Definition of the non-proportionality factor $\mathbf{F_{NP}}$ for proportional (left), **90°** out-of-phase (middle), and general tension-torsion stress histories (right) (1).

The general periodic tension-torsion path exemplified in Fig. 2(right) is a combination of an outer and an inner loop that results in two different loading cycles per period, therefore it can be classified as a variable amplitude loading (VAL) history. On the other hand, periodic paths consisting of one cycle per period, such as the proportional and the **90°** out-of-phase examples from Fig. 2, are classified as constant amplitude loading (CAL) histories. Naturally, any non-periodic and non-monotonic load path results in a VAL history.

Notice that in-phase or **180°** out-of-phase loads can result in NP histories, as seen in the straight path **C** in Fig. 3, which has a variable $\tau_{xy}(t)/\sigma_x(t)$ ratio, thus variable principal directions. However, the straight path **B**, which is also in-phase and with a non-zero mean load, induces a proportional load history because it maintains a fixed $\tau_{xy}(t)/\sigma_x(t)$ ratio, similarly to path A. Load phase and load proportionality are indeed different concepts.

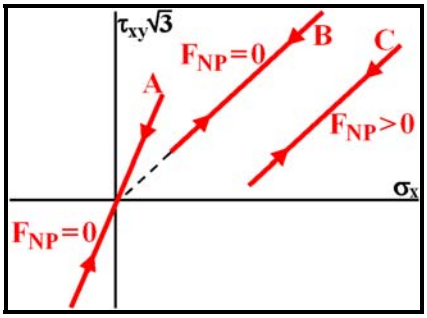


Fig. 3: In-phase tension-torsion stress paths that result in proportional histories for paths **A** and **B** and in a NP history for **C**.

However, both in-phase or out-of-phase biaxial tension-compression histories induced by perpendicular loads are always proportional, since they maintain fixed principal-stress directions and thus induce $\tau_{xy}(t) \equiv 0 \Rightarrow d\theta_1(t)/dt = 0$, see Fig. 4. This is the reason why NP experiments should be performed on tension-torsion testing machines instead of biaxial load frames with two perpendicular jacks, which cannot induce NP loads.

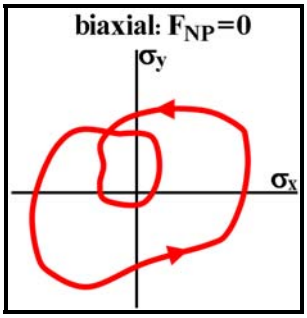


Fig. 4: General biaxial history, which is always proportional in the absence of shear stresses.

The simple examples discussed above involve histories with only two stress components. For general six-dimensional (6D) stress histories, the $\mathbf{F_{NP}}$ estimates need to consider the path of all six stress components $\sigma_x$, $\sigma_y$, $\sigma_z$, $\tau_{xy}$, $\tau_{xz}$ and $\tau_{yz}$. Fatigue crack initiation assessments require as well the use of damage models based on methodologies that depend on the material type, as discussed next.

*Directional-damage materials*, like most metals, fail by fatigue due to a *single dominant crack*. The plane along which the microcrack initiates at the critical point is called the *critical plane*, whose direction must be estimated using multiaxial fatigue damage models that take into account the stress and strain histories projected onto it. For such materials, it is usual to neglect fatigue damage eventually induced on other planes, assuming they do not interact or affect the microcrack initiation

process on the critical plane. It is also assumed that fatigue damage can be properly evaluated based only on the normal and shear stress (and/or strain) histories acting on the critical plane. It is important to note that the plane where the microcrack initiates (the critical plane) may be (and usually is) different from the plane where the resulting macroscopic fatigue crack propagates. For modeling purposes, the search for the critical-plane direction can be performed using so-called critical-plane approaches.

*Distributed-damage materials*, on the other hand, fail by multiaxial fatigue due to *distributed mechanisms*, which may cause e.g. multiple cracking in concrete or distributed cavitations in ductile metals under high loads. Fiber-reinforced composites fail by distributed mechanisms as well, because fiber unsticking and rupture happen along their multiple directions, so they usually need to be described by anisotropic damage models. Moreover, even though multiple microcracks (in concrete) and fiber failure (in composites) can happen in several different directions, all of them can contribute altogether to the accumulated damage in such materials, as well as to the decrease or loss of their stiffness. Consequently, significant interaction among damage mechanisms acting on different planes and directions can happen in these distributed-damage materials, as opposed to what happens in directional-damage materials. Multiaxial fatigue damage evaluations in distributed-damage materials usually involve invariants like the von Mises and the hydrostatic components, which are able to mix stress and/or strain contributions in all directions, without assuming a preferential plane.

## EQUIVALENT STRESSES AND STRAINS

Several yielding, failure, and fatigue criteria are based on comparisons between a uniaxial strength and an equivalent stress or strain that combines all multiaxial components. The most widely used model to calculate such equivalent stresses and strains is the von Mises yield criterion. The loading parameter in fatigue crack initiation models for these materials can be the von Mises equivalent stress $\sigma_{Mises}$, shear stress $\tau_{Mises}$, or else the octahedral shear stress $\tau_{oct}$.

However, as $\sigma_{Mises}$ and $\tau_{Mises}$ are always positive, they cannot identify whether a load cycle is tensile or compressive, a major issue in fatigue analyses. Indeed, two simple uniaxial stress states $\sigma_{x1} = 200MPa$ and $\sigma_{x2} = -200MPa$ both have the same $\sigma_{Mises} = 200MPa$, wrongfully suggesting that an alternate loading between $\sigma_{x1}$ and $\sigma_{x2}$ would be constant despite its sign change.

To avoid this problem, a von Mises equivalent stress range $\Delta\sigma_{Mises}$ (also called relative von Mises stress $\sigma_{RMises}$) can be used in cyclic or VAL histories to correctly evaluate the variation of $\sigma_{Mises}$ along the loading path, caused by the stress range components $(\Delta\sigma_x, \Delta\sigma_y, \Delta\sigma_z, \Delta\tau_{xy}, \Delta\tau_{xz}, \Delta\tau_{yz})$, calculated from:

$$\Delta\sigma_{Mises}^2 = \frac{(\Delta\sigma_x - \Delta\sigma_y)^2}{2} + \frac{(\Delta\sigma_x - \Delta\sigma_z)^2}{2} + \frac{(\Delta\sigma_y - \Delta\sigma_z)^2}{2} + 3(\Delta\tau_{xy}^2 + \Delta\tau_{xz}^2 + \Delta\tau_{yz}^2) \quad (2)$$

Such relative von Mises ranges are easy to obtain for proportional load histories, from the differences between the maximum and minimum values of each stress component. However, for NP load histories such relative ranges are not able to consider the significant load path shape influence on fatigue life, as discussed next. Moreover, invariants such as von Mises are only applicable for distributed-damage materials, unless the load history is very simple for such a differentiation not to matter. Despite these limitations, some codes are still based on invariants, as discussed next.

## THE ASME BOILER AND PRESSURE VESSEL CODE

The ASME Boiler and Pressure Vessel Code (2) is a widely used design tool that includes a method to estimate equivalent stresses (or strains) from arbitrary multiaxial load paths at critical points, usually notch tips. Such load paths can either represent an entire period of a periodic CAL history, or a half-cycle from a VAL history counted using a multiaxial rainflow method such as the Modified Wang-Brown (3).

However, this traditional code has some idiosyncrasies, e.g. its equivalent stresses are calculated by Tresca, while its equivalent strain equations adopt the von Mises criterion. For simplicity, the von Mises criterion is used below for both equivalent stress and strain calculations, which is less computationally intensive than the Tresca version, while giving similar results.

For a stress path at the critical point given by the time histories $\sigma_x(t)$, $\sigma_y(t)$, $\sigma_z(t)$, $\tau_{xy}(t)$, $\tau_{xz}(t)$, and $\tau_{yz}(t)$, the ranges between any two instants $t = t_1$ and $t = t_2$ along the load path are defined as

$$\begin{cases} \Delta\sigma_x(t_1,t_2) \equiv \sigma_x(t_2) - \sigma_x(t_1) \\ \Delta\sigma_y(t_1,t_2) \equiv \sigma_y(t_2) - \sigma_y(t_1) \\ \Delta\sigma_z(t_1,t_2) \equiv \sigma_z(t_2) - \sigma_z(t_1) \end{cases} \quad (3)$$
$$\begin{cases} \Delta\tau_{xy}(t_1,t_2) \equiv \tau_{xy}(t_2) - \tau_{xy}(t_1) \\ \Delta\tau_{xz}(t_1,t_2) \equiv \tau_{xz}(t_2) - \tau_{xz}(t_1) \\ \Delta\tau_{yz}(t_1,t_2) \equiv \tau_{yz}(t_2) - \tau_{yz}(t_1) \end{cases}$$

The von Mises shear stress range $\Delta\tau_{Mises}$ is then obtained from the two instants $t = t_1$ and $t = t_2$ where its expression is maximized, i.e.

$$\Delta\tau_{Mises}^2 = \max_{t_1,t_2} \left\{ \Delta\tau_{xy}^2 + \Delta\tau_{xz}^2 + \Delta\tau_{yz}^2 + \frac{(\Delta\sigma_x - \Delta\sigma_y)^2}{6} + \frac{(\Delta\sigma_x - \Delta\sigma_z)^2}{6} + \frac{(\Delta\sigma_y - \Delta\sigma_z)^2}{6} \right\} \quad (4)$$

The von Mises equivalent stress range is then calculated from $\Delta\sigma_{Mises} = \Delta\tau_{Mises} \cdot \sqrt{3}$.

An analogous procedure can be adopted for strain paths given by the time histories $\varepsilon_x(t)$, $\varepsilon_y(t)$, $\varepsilon_z(t)$, $\gamma_{xy}(t)$, $\gamma_{xz}(t)$, and $\gamma_{yz}(t)$, defining the ranges

$$\begin{cases} \Delta\varepsilon_x(t_1,t_2) \equiv \varepsilon_x(t_2) - \varepsilon_x(t_1) \\ \Delta\varepsilon_y(t_1,t_2) \equiv \varepsilon_y(t_2) - \varepsilon_y(t_1) \\ \Delta\varepsilon_z(t_1,t_2) \equiv \varepsilon_z(t_2) - \varepsilon_z(t_1) \\ \Delta\gamma_{xy}(t_1,t_2) \equiv \gamma_{xy}(t_2) - \gamma_{xy}(t_1) \\ \Delta\gamma_{xz}(t_1,t_2) \equiv \gamma_{xz}(t_2) - \gamma_{xz}(t_1) \\ \Delta\gamma_{yz}(t_1,t_2) \equiv \gamma_{yz}(t_2) - \gamma_{yz}(t_1) \end{cases} \quad (5)$$

from which the von Mises shear strain range $\Delta\gamma_{Mises}$ is calculated from the maximization problem

$$\Delta\gamma_{Mises}^2 = \max_{t_1,t_2} \left\{ \Delta\gamma_{xy}^2 + \Delta\gamma_{xz}^2 + \Delta\gamma_{yz}^2 + \frac{2}{3} \cdot [(\Delta\varepsilon_x - \Delta\varepsilon_y)^2 + (\Delta\varepsilon_x - \Delta\varepsilon_z)^2 + (\Delta\varepsilon_y - \Delta\varepsilon_z)^2] \right\} \quad (6)$$

where the von Mises equivalent strain range is obtained from $\Delta\varepsilon_{Mises} = \Delta\gamma_{Mises} \cdot \sqrt{3}/[2 \cdot (1+\bar{\nu})]$, where $\bar{\nu}$ is the elastoplastic Poisson ratio that combines elastic and plastic effects defined as $\bar{\nu} = (\nu \cdot \varepsilon_{el,Mises} + 0.5 \cdot \varepsilon_{pl,Mises})/(\varepsilon_{el,Mises} + \varepsilon_{pl,Mises})$, whose value lies in-between the elastic ($\nu$) and plastic ($0.5$) Poisson ratios, i.e. $\nu \le \bar{\nu} \le 0.5$ (4).

For a simple multiaxial proportional CAL history, this method results in a von Mises equivalent range calculated from the difference between the peak and the valley of the considered load cycle.

However, for general multiaxial NP load histories, where the principal stress directions can vary, the approach adopted by the ASME B&PV code can result in highly *non-conservative* predictions. For instance, all four stress paths illustrated in the $\sigma_x \times \tau_{xy}\sqrt{3}$ diagram depicted in Fig. 5 (one proportional with no shear components, two elliptical with different $\tau_{max}/\sigma_{max}$ ratios, and one circular with $\tau_{max}\sqrt{3}/\sigma_{max} = 1$) would be associated with the very same von Mises equivalent stress range $\Delta\sigma_{Mises} = L$ according to the simplified procedures recommended by the ASME code, because Eq. (4) is maximized (in all four cases) for the instants $t_1$ and $t_2$ where $\sigma_x = \pm L/2$ and $\tau_{xy} = 0$, where $L$ is the longest chord in the load history diagram.

However, the fatigue damage induced by the circular stress path in Fig. 5 should be significantly higher than the damage induced by the proportional (uniaxial) stress path, whereas the damage induced by the elliptical stress paths increase as their $F_{NP}$ increases. Several experiments (5) have shown that longer stress paths associated with NP loads are significantly more damaging than straight proportional paths.

For instance, the ASME B&PV code can non-conservatively *underestimate* by a factor of $\sqrt{3}$ the equivalent von Mises range of the circular stress path from Fig. 5, when compared to the more reasonable $\Delta\sigma_{Mises} = L\sqrt{3}$ predicted from the MOI (moment of inertia) method for estimating equivalent amplitudes of non-proportional multiaxial stress or strain histories (6). Or else, based on the theory of convex enclosures of NP stress paths (7), the ASME B&PV code can also *underestimate* the equivalent von Mises range of circular paths by a factor of $\sqrt{2}$ when compared to the $\Delta\sigma_{Mises} = L\sqrt{2}$ predicted from most convex-enclosure methods.

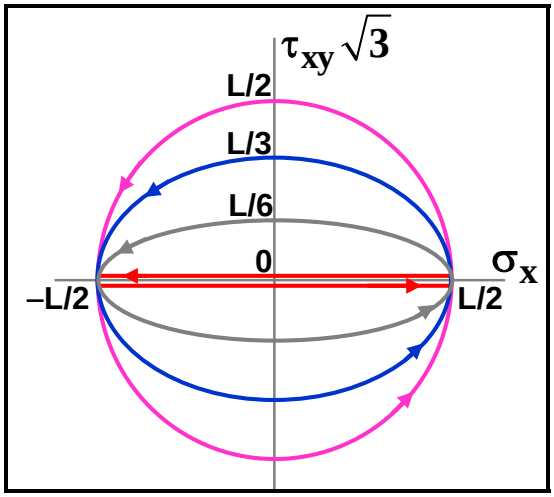


Fig. 5: Proportional, elliptical, and circular stress paths in the $\sigma_x \times \tau_{xy}\sqrt{3}$ diagram would result in the same von Mises equivalent stress range $\Delta\sigma_{Mises} = L$ according to the ASME standard procedures, a prediction that is highly non-conservative.

In fact, experimental evidence and convex enclosure methods (7) show that the $90^o$ out-of-phase tension-torsion circular path from Fig. 5 should be associated with an equivalent $\Delta\sigma_{Mises}$ much larger than the $L$ range proposed by the ASME B&PV code, typically between $L\sqrt{2}$ and $L\sqrt{3}$. Since such larger equivalent $\Delta\sigma_{Mises}$ values are of course associated with much shorter fatigue lives, the ASME B&PV code procedures are indeed *non-conservative*, hence they probably should be reviewed. The elliptical stress paths in Fig. 5 should have $\Delta\sigma_{Mises}$ in-between the circular path value and the value $\Delta\sigma_{Mises} = L$ from the proportional horizontal path shown in the figure, however this effect is completely ignored by the ASME code procedures as well.

It can be concluded that since the procedure used by the ASME B&PV code does not take into account the shape of the multiaxial stress path, it only considers the maximum stress range within it. Hence, it can be regarded as a "longest chord" approach. This simplistic approach searches for the longest straight line joining two points from the stress path represented in the deviatoric stress space, whose length $L$ would be assumed as the equivalent stress range $\Delta\sigma_{Mises} = L$ without any

correction to account for the path shape. The same conclusions can be drawn for ASME's $\Delta\varepsilon_{Mises}$ estimates, which would search for the longest chord in the strain path represented in the deviatoric strain space.

These *non-conservative* ASME B&PV code predictions are almost identical to the ones obtained from the pioneer Dang Van's Minimum Ball procedure (8), which would circumscribe the same circle with diameter **L** to all four load paths from Fig. 5, regardless of their different proportional or NP natures, wrongfully estimating like the ASME code the same equivalent stress range $\Delta\sigma_{Mises} = \mathbf{L}$ for all of them.

For NP histories, it is thus recommended to adopt some path-equivalent procedure such as the MOI method (6) to calculate $\Delta\sigma_{Mises}$ for distributed-damage materials. On the other hand, for NP histories on directional-damage materials (such as most metallic alloys), a combination of the MOI and the critical plane approach is required to consider the directional nature of initiating cracks. Details on the implementation of the critical plane approach can be found in (4) and (9-10).

Finally, the ASME B&PV code procedures assumes that all loads are CAL, since no cycle counting method is adopted or proposed to account for fatigue damage. However, to deal with VAL histories it is also necessary to apply a multiaxial rainflow counting procedure before calculating fatigue damage, such as the one detailed in (3). This is an important issue that probably should also be reviewed in the calculation routines adopted by the ASME code.

## CONCLUSIONS

In this work, some multiaxial fatigue procedures proposed by the ASME Boiler and Pressure Vessel Code were critically reviewed. It was concluded that the ASME method should only be used for proportional or nearly proportional multiaxial load histories. Moreover, it should only be applied with invariant-based fatigue damage estimations, since $\Delta\sigma_{Mises}$ or $\Delta\varepsilon_{Mises}$ mix all stress or strain components without considering the direction of the plane where the microcrack initiates at the critical point. Such invariant-based calculation procedures should not be used for directional-damage materials like the metallic alloys used in the vessels, because they do not account for the physics of the cracking problem in such materials, which fail by fatigue by the propagation of a dominant crack, not by distributed damage. Indeed, the von Mises equivalent ranges proposed by the ASME code mix stresses or strains from different planes, a procedure that is incompatible with the critical-plane approaches needed to describe fatigue damage in such materials.

## ACKNOWLEDGMENTS

This work was supported in part by the National Natural Science Foundation of P.R. China under Grant No. 11302150. CNPq-Brazil provided research fellowship for Prof. Marco A. Meggiolaro.

## REFERENCES

(1) Socie,DF; Marquis,GB. Multiaxial Fatigue. SAE, 2000.

(2) ASME Boiler and Pressure Vessel Code, Section III: Rules for construction of nuclear facility components, Division 1, Subsection NB: Class 1 components, ASME 2013.

(3) Meggiolaro,MA; Castro,JTP. An improved multiaxial rainflow algorithm for non-proportional stress or strain histories - part II: the modified Wang-Brown method. Int J Fatigue 42:194-206, 2012.

(4) Castro, J.T.P., Meggiolaro, M.A. Fatigue Design Techniques v. 2: Low-Cycle and Multiaxial Fatigue. CreateSpace 2016.

(5) Itoh,T; Sakane,M; Ohnami,M; Socie,DF. Nonproportional low cycle fatigue criterion for type 304 stainless steel. J Eng Mater Technol 117:285-292, 1995.

(6) Meggiolaro, M.A., Castro, J.T.P., Wu, H., "Generalization of the Moment Of Inertia method to predict equivalent amplitudes of non-proportional multiaxial stress or strain histories", Acta Mechanica 227(11):3261-3273, 2016.

(7) Meggiolaro,MA; Castro,JTP. An improved multiaxial rainflow algorithm for non-proportional stress or strain histories - part I: enclosing surface methods. Int J Fatigue 42: 217-226, 2012.

(8) Dang Van,K; Griveau,B; Message,O. On a new multiaxial fatigue limit criterion: theory and application. In: Biaxial and Multiaxial Fatigue, EGF3:479-496, 1989.

(9) Bannantine,JA; Socie,DF. A variable amplitude multiaxial fatigue life prediction method. Fatigue Under Biaxial and Multiaxial Loading, ESIS publ. 10:35-51, 1991.

(10) Rettenmeier,P; Herter,K-H; Schuler,X; Fesich,T.M. Application of Advanced Fatigue Damage Parameters in Comparison With Fatigue Analysis Included in Codes and Standards. ASME 2014 Pressure Vessels and Piping Conference.